



HAL
open science

High methane potential of oxygenic photogranules decreases after starvation

Sandra Galea-Outón, Kim Milferstedt, Jérôme Hamelin

► To cite this version:

Sandra Galea-Outón, Kim Milferstedt, Jérôme Hamelin. High methane potential of oxygenic photogranules decreases after starvation. *Bioresource Technology*, 2024, 406, pp.110986. 10.1016/j.biortech.2024.130986 . hal-04677885

HAL Id: hal-04677885

<https://hal.inrae.fr/hal-04677885v1>

Submitted on 26 Aug 2024

HAL is a multi-disciplinary open access archive for the deposit and dissemination of scientific research documents, whether they are published or not. The documents may come from teaching and research institutions in France or abroad, or from public or private research centers.

L'archive ouverte pluridisciplinaire **HAL**, est destinée au dépôt et à la diffusion de documents scientifiques de niveau recherche, publiés ou non, émanant des établissements d'enseignement et de recherche français ou étrangers, des laboratoires publics ou privés.



Distributed under a Creative Commons Attribution 4.0 International License



High methane potential of oxygenic photogranules decreases after starvation

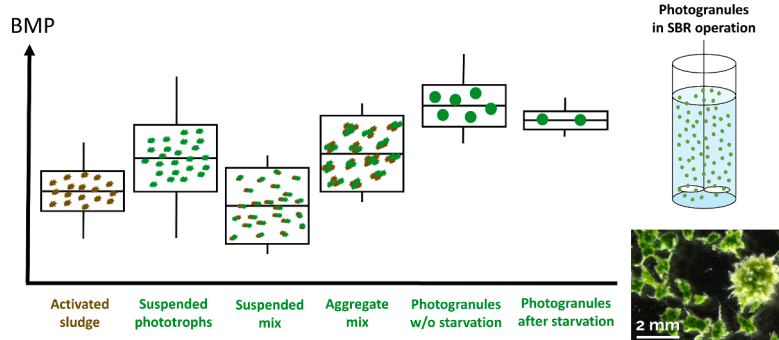
Sandra Galea-Outón, Kim Milferstedt¹, Jérôme Hamelin^{*,1}

INRAE, Univ Montpellier, LBE, 102 Avenue des étangs, 11100 Narbonne, France

HIGHLIGHTS

- Oxygenic photogranules (OPG) has high biochemical methane potential (BMP)
- BMP of OPG based on near-infrared spectrum is as accurate as traditional BMP tests.
- BMP of OPG biomass was cut by about 20 % after a starvation period of 3 days.
- Reactor operating conditions can modulate the energy recovery from OPG.

GRAPHICAL ABSTRACT



ARTICLE INFO

Keywords:

Phototrophic-heterotrophic syntrophy
SBR
Wastewater treatment
Anaerobic digestion
Circular economy
Biorefinery

ABSTRACT

Oxygenic photogranules (OPG) are granular biofilms that can treat wastewater without external aeration, making it an advantage over activated sludge. Excess of OPG biomass can serve as energy source through anaerobic digestion. Two sequencing batch photoreactors were operated over 400 days to grow OPG. Biochemical methane potentials (BMP) were obtained from near-infrared spectroscopy. OPGs had an average BMP of 356 mL CH₄·gVS⁻¹, much higher than typical BMP from activated sludge. A partial least squares analysis could relate BMP with reactor operating conditions, like light regime, load or biomass concentration. Since organic load was the most influential parameter on BMP, three starvation experiments were set up. An average decrease of BMP by 18.4 % was observed. However, the unexpected growth of biomass during starvation resulted in a higher total methane volume. In conclusion, starvation reduces the BMP of OPGs but anaerobic digestion of OPG biomass remains a promising route for biomass valorization.

1. Introduction

The United Nations sustainable development goal “Responsible consumption and production” fosters a more efficient use of the

resources and the recovery of value-added products to promote a circular use of matter. This applies also to wastewater treatment. A step towards a circular use of resources is taken by the aerobic granule technology as a promising alternative to the commonly used

* Corresponding author at: INRAE, Univ Montpellier, LBE, 102 Avenue des étangs, 11100 Narbonne, France.

E-mail address: jerome.hamelin@inrae.fr (J. Hamelin).

¹ These authors contributed equally to this work.

conventional activated sludge (CAS) process for wastewater treatment (van der Roest et al., 2011; Pronk et al., 2015). While value-added products can be recovered from aerobic granules, the wastewater treatment process still mainly relies on the oxidation of carbon compounds and releases CO₂ into the atmosphere. The required oxygen is provided by mechanical aeration. This drawback may be overcome by another member of the family of granulated biomass: oxygenic photogranules. OPGs produce oxygen in situ and CO₂ may be incorporated into the biomass through photosynthesis by the phototrophic members of the OPG community (Milferstedt et al., 2017). External aeration may therefore become unnecessary, reducing operating expenses (Brockmann et al., 2021). OPGs may be a candidate biomass for a future wastewater treatment with a reduced environmental impact.

Incorporation of additional CO₂ into biomass is responsible for a higher biomass yield of an OPG process and leading to the production of larger quantities of excess sludge compared to aerobic granules and activated sludge. Processing a higher amount of excess sludge creates additional costs. Already during wastewater treatment by conventional activated sludge process, a technology with a comparably low sludge yield, half of the operating costs of a wastewater treatment plant are generated by sludge handling (Appels et al., 2008). Consequently, it is of interest for the sustainability of the process to identify uses for the excess biomass (Brockmann et al., 2021).

One common process to treat excess activated sludge is anaerobic digestion. Anaerobic digestion describes the fermentation of organic material contained in sludge. It generates biogas, a mixture containing approximately 60 % CH₄ and 40 % CO₂. Biogas can be used as an energy vector to generate heat and electricity directly in the treatment plant or elsewhere. Biogas can also be generated from the digestion of OPG biomass. However, little data is available on the digestibility of OPG biomass. Most of the phototrophic biomass within OPGs is filamentous cyanobacteria (such as *Oscillatoria sp.*) (Milferstedt et al., 2017), but there is also microalgae. Microalgae possess a cell wall that is comparably difficult to break. For that reason, microalgae biomass often requires costly pretreatment to produce economically and ecologically acceptable quantities of biogas during digestion. Therefore, the phototrophic cells of the microbial community might make the estimation of methane yield from OPGs difficult. Not only the microbial composition of OPGs may have an effect on the digestibility of the biomass, but also the composition of the biomass itself, e.g., its protein, carbohydrate and lipid content. A drastic change in operational conditions, e.g., a starvation period, may change the proportions of the cellular components and consequently influence the digestibility of the biomass. In the literature, a broad characterization of the digestibility of this new type of biomass is currently lacking and will be provided in this study.

A commonly used tool to assess the digestibility of any kind of biomass is the biochemical methane potential (BMP) test that quantifies the maximum amount of methane produced by anaerobic digestion for a unit of biomass (Angelidaki et al., 2009). Alternatively, the BMP can be measured by near-infrared spectroscopy (NIRS) using commercially available methods.

Based on various published articles, an average BMP of 219 ± 54 mL CH₄·gVS⁻¹ can be calculated for activated sludge (Supplementary material). Park et al. (2015) published with 230 mL CH₄·gVS⁻¹ the so far only available BMP for photogranules. However, for other types of microalgae-bacteria biomass, values up to 348 mL CH₄·gVS⁻¹ are reported (Arcila and Buitrón, 2016). This rather high range of values makes it necessary to measure BMP for photogranules from various sources and subjected to contrasted environmental conditions to establish a more solid basis of the BMP that can be expected from this novel kind of biomass.

In this study, two sequencing batch reactors (SBR) were operated to produce OPG biomass from a synthetic wastewater. The reactors were operated for more than 400 days under varying operating conditions. Biomass was systematically sampled and its BMP was predicted. The resulting BMPs were correlated to operating conditions and notably the

exposure to starvation. It was hypothesized that starvation has a notable effect on BMP as the biomass composition is likely to change as a function of nutrient availability.

2. Material and methods

2.1. Reactor operation

Two sequencing batch photobioreactors (SBR-1 and SBR-2) were operated for a period of more than 400 days. The working volume in the reactors was four liters. During each SBR cycle, two liters and thus half of the volume was replaced with fresh media. For most part of the experiment, the reactors were operated at a cycle length of four hours, resulting in a hydraulic retention time (HRT) of 8 h. At day 329 until the end of reactor operation, the cycle length was decreased to three hours with a resulting HRT of 6 h. A cycle consisted of (1) six minutes filling, (2) 171 or 231 min reaction time (three- or four-hour cycles, respectively), (3) 0,5 min settling, (4) 2,5 min emptying (Fig. 1A).

2.2. Environmental conditions

The reactors received a synthetic wastewater as feed with a carbon load of 48.8, 24.4, 21.7 or 16.2 mg COD·L⁻¹·h⁻¹, depending on the phase of the experiment (Fig. 1C). The composition and concentrations of the feed solution were as follows: 6.1 mM sodium acetate (390 mg COD·L⁻¹), 1.52 mM (NH₄)₂SO₄, 70 μM KH₂PO₄, 60 μM Na₂HPO₄, 13.43 μM EDTA·Na₂, 2.47 μM FeCl₃, 10 nM Na₂MoO₄, 70 nM FeSO₄, 490 nM H₃BO₃, 30 nM ZnSO₄, 20 nM MnCl₂, 80 nM CoCl₂, 120 nM CuSO₄ and 10 nM NiCl₂.

The reactors were illuminated using LED panels of white light (4000 K). When illuminated, the LED panels produced on average a photosynthetically active radiation (PAR) of 62 or 96 μmol·m⁻²·s⁻¹ at the vertical surfaces of the reactors during conditions 1 and 2, and conditions 3 to 5, respectively (Fig. 1B). Light was switched off for 30 min at the end of four-hour cycles and 15 min at the end of three-hour cycles (Fig. 1A). Therefore, over a day with three-hour and four-hour cycles (conditions 4 and 5, and conditions 1 to 3), the reactors received a daily dose of 4.7, 7.2 and 7.6 mol·m⁻² of PAR per day under conditions 1 and 2, condition 3 and conditions 4 and 5, respectively (Fig. 1B).

Both reactors were operated at an average room temperature of 25 °C. A sufficiently large and naturally ventilated distance between LED panels and the reactors insured that the temperature in reactors was not affected by the LED panels. The reactor content was mixed using an overhead stirrer at 100 rpm. The average pH in the reactor was 8. Temperature and pH in the reactors were monitored online but were not controlled.

In consecutive experiments, several correlated operational parameters were varied so that the influence of these parameters on the BMP of the resulting biomass could be tested statistically. The parameters HRT, load, initial soluble COD ('maxCOD') and biomass concentration (as total suspended solids, TSS) were independent of each other. Light regime ('PAR per day') was treated as independent from light intensity ('PAR') because of the dark phase at the end of each SBR cycle. The parameters cycle length as well as light-timing (that determines light regime) correlate with a correlation coefficient of 1 with HRT; total solids, volatile solids, and volatile suspended solids correlated with total suspended solids with a correlation coefficient of 0.8 (p-value < 0.001). Therefore, these parameters were not included in the analysis, as they do not add explanatory power to the PLS model, but make it more complex. In total, five combinations of the independent parameters were obtained ('Conditions' indicated in Fig. 1B) that are listed in Table 1 and were used in the PLS model.

2.3. Biomass collection and sample preparation

The biomass in the two reactors was composed of oxygenic photogranules in a size range from 0.5 to 4 mm in diameter. The biomass

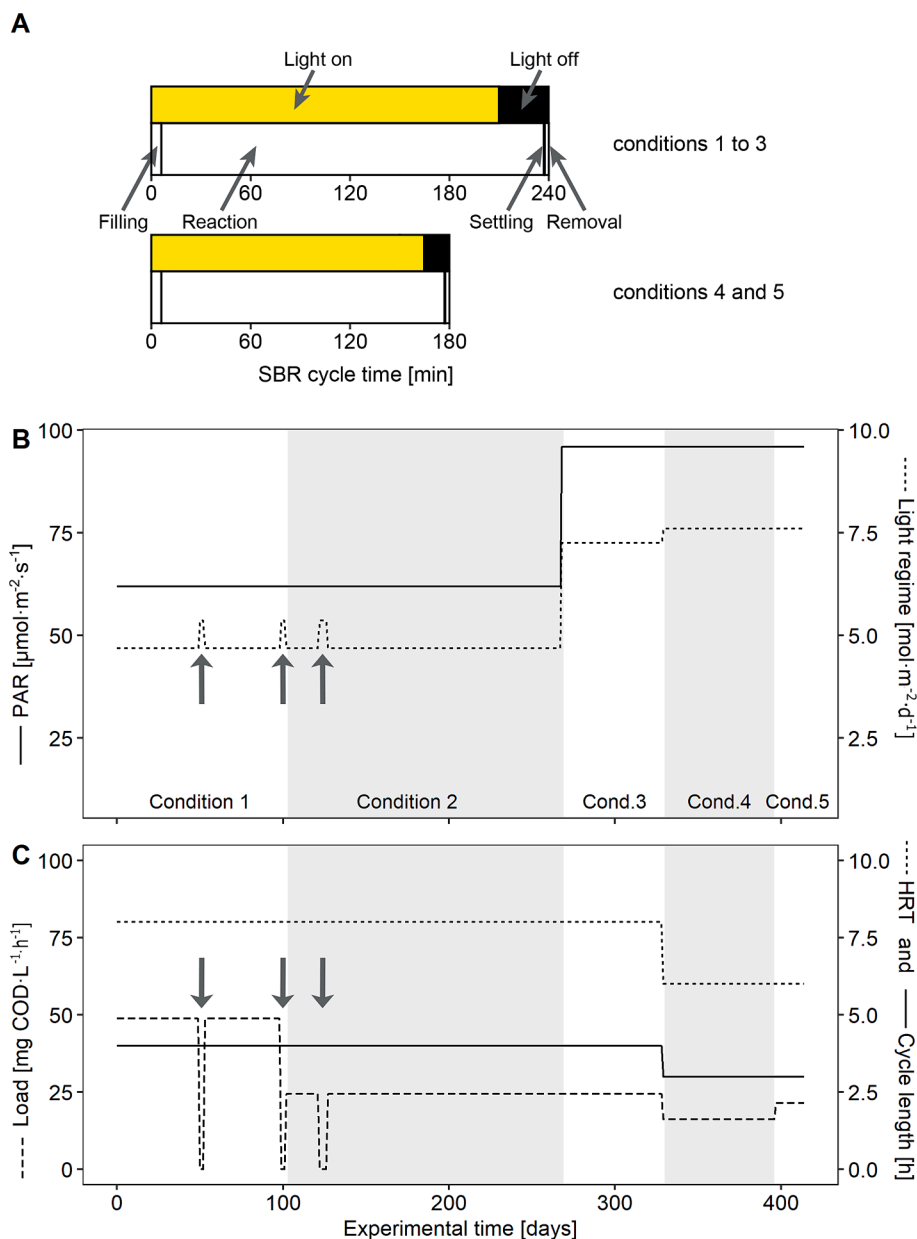


Fig. 1. Operating conditions for the two sequencing batch reactors (SBR). (A) The SBR cycles including illumination. (B) Illumination over the duration of the experiment with the average light at the vertical surfaces of the reactors (photosynthetic active radiation, PAR) and the daily light dose, taking into account the dark phases at the end of the SBR cycles (light regime). (C) Cycle length, hydraulic retention time (HRT) and carbon load over the duration of the experiment. Additionally, arrows in panels B and C signal to starvation experiments.

concentration as total suspended solids (TSS) was measured according to Standard Methods 2540D (Lipps et al., 2017). From the same biomass, 55 samples were collected and used for NIRS BMP analysis. Samples were always taken at the end of a cycle when the dissolved oxygen in the bulk phase was increasing. Measurable dissolved oxygen in the bulk phase correlated with a soluble COD concentration approaching zero. This was experimentally verified. To account with heterogeneity in the photogranule population, one large sample containing between 25 and 50 % of the total biomass in the reactors was collected per reactor at each sampling date. The large sampling mass was also taken to adjust the sludge concentration in the reactors. The reactors continued normal operation after sampling and no deterioration of carbon removal was observed. Ammonium and EPS concentrations were not measured during the experiment.

Additionally, nine samples of monoclonal cultures of cyanobacteria were taken for NIRS BMP analysis from the culture collection of this

study. The strains were isolated from OPGs in a previous study. Monoclonal cyanobacteria were cultured in sterile flasks that allows gas exchange, with standard BG-11 medium for cyanobacteria cultivation, exposed to $100 \mu\text{mol}\cdot\text{m}^{-2}\cdot\text{s}^{-1}$ PAR and at room temperature.

All samples were then centrifuged for 1 min at 7000 g (Eppendorf Centrifuge 5430, Hamburg, Germany) and the liquid fraction was removed. To preserve the samples, they were freeze-dried and ground, yielding between 3 and 6 g of a fine powder. The samples were stored at room temperature in the dark before analyses.

2.4. Starvation experiments

Six additional biomass samples were collected after starvation periods of three days and processed as detailed above. The three independent experiments were carried out at an interval of 45 days between the first and second, and 25 days between the second and third

Table 1
Combination of parameters tested for PLS statistical analysis.

| - | Organic carbon | | HRT (h) | Light intensity | | TSS (g·L ⁻¹) | Nb |
|---|---------------------------|--|------------|--|------------------------|-----------------------------|----|
| | Feed | Load | | PAR | PAR per day | | |
| | (mg COD·L ⁻¹) | (mg COD·L ⁻¹ ·h ⁻¹) | | (μmol·m ⁻² ·s ⁻¹) | (mol·m ⁻²) | | |
| 1 | 195.0 | 48.8 | 8 | 62 | 4.7 | 4.3 – 9.2 | 14 |
| 2 | 97.5 | 24.4 | 8 | 62 | 4.7 | 1.6 – 12.5 | 22 |
| 3 | 97.5 | 24.4 | 8 | 96 | 7.2 | 1.9 – 5.0 | 4 |
| 4 | 48.8 | 16.2 | 6 | 96 | 7.6 | 3.3 – 6.4 | 10 |
| 5 | 65.0 | 21.7 | 6 | 96 | 7.6 | 3.5 – 9.3 | 5 |

Note: Nb: the number of samples taken under the defined conditions. 'HRT' stands for hydraulic retention time; 'PAR' stands for photosynthetic active radiation; 'TSS' stands for total suspended solids; 'COD' stands for chemical oxygen demand.

starvation periods. It is assumed that the intervals allowed the recovery of storage compounds.

For each of the starvation periods, a reduced COD load was manually added three times per day, containing 16 % or 8.0 mg COD·L⁻¹·h⁻¹ during the first starvation experiment, 11 % or 5.4 mg COD·L⁻¹·h⁻¹ during the second starvation experiment, and 0 % of the initial load during the third starvation experiment (Table 2). The progressive reduction was done to reduce the risk of reactor failure. During starvation, light was constantly supplied to maximize oxidation of available COD, i.e., it was not turned off for 30 min as during normal operation, resulting in 5.4 mol·m⁻² of PAR per day instead of 4.7 mol·m⁻² of PAR per day. In addition to oxygen provided by photosynthesis, external aeration was supplied to provide dissolved oxygen concentrations at air saturation (9 mg·L⁻¹), before every manual feeding. The supplemental oxygen guaranteed that oxygen did not become limiting. Heterotrophic activity was thus sustained and the depletion of soluble carbon sources was achieved for every reactor cycle.

2.5. Near-Infrared spectroscopy

The NIRS method is based on a statistical model trained with a large number of conventional BMP measurements, including phototrophic biomass. A conventional BMP test is labor intensive, takes about one month and requires biomass on the order of several grams. Results from traditional BMP tests may highly vary between laboratories, despite international efforts of standardization (Holliger et al., 2016). The main advantages of NIRS, comparing with traditional BMP tests, are its rapidity and the non-destructive use of small amounts of biomass (2 cm³ of freeze-dried biomass).

BMP predictions for the lyophilized and ground biomass were done for all samples taken during the whole experiment (Fig. 2) using the commercially available near-infrared spectroscopy (NIRS) method Flash BMP® 11,059,628 by Büchi, integrated in the software for the BUCHI NIR-Flex N-500 solids spectrophotometer (Buchi, Flawil, Switzerland). Details on the NIRS method are given in Lesteur et al. (2011) and Latrille et al. (2013). A disadvantage of the NIRS method is the risk that the biomass to be tested is not represented in the database used to calculate

Table 2
Operating conditions of SBRs before and during the three starvation experiments and characteristics of OPG biomass observed before and after starvation.

| Exp. | SBR | Load (mg COD·L ⁻¹ ·h ⁻¹) | | VSS (g·L ⁻¹) | | C/N | | BMP (mL CH ₄ ·g ⁻¹ VS) | |
|------|-----|--|------------|-----------------------------|------------|--------|-------|---|-------|
| | | before | starvation | before | after | before | after | before | after |
| | | 1 | 1 | 48.8 | 8.0 (16 %) | 0.4 | 0.6 | 3.3 | 3.7 |
| 1 | 2 | 48.8 | 8.0 (16 %) | 1.0 | 0.4 | 3.8 | 3.3 | 450 | 361 |
| 2 | 1 | 48.8 | 5.4 (11 %) | 1.6 | 1.9 | 5.1 | 5.3 | 523 | 519 |
| 2 | 2 | 48.8 | 5.4 (11 %) | 1.6 | 1.2 | 5.5 | 5.9 | 518 | 322 |
| 3 | 1 | 24.4 | 0 (0 %) | 1.1 | 2.2 | 4.2 | 2.9 | 337 | 289 |
| 3 | 2 | 24.4 | 0 (0 %) | 0.8 | 2.3 | 4.5 | 3.4 | 303 | 247 |

Note: 'Exp.' stands for experiment number; 'SBR' stands for sequencing batch reactor; 'COD' stands for chemical oxygen demand; 'VSS' stands for volatile suspended solids; 'C/N' stands for carbon to nitrogen ratio; 'OPG' stands for oxygenic photogranules; 'BMP' stands for biochemical methane potential; and 'VS' stands for volatile solids.

the BMP from the spectra. This problem can be addressed by running a comparison between a NIRS prediction with a biological BMP of a type biomass, as done in this study. The validity of the NIRS method was confirmed in a comparison with the result obtained from a photogranule biomass using the traditional BMP test. The two results differed by 3.3 %.

NIRS was also used to predict the macromolecular composition of the biomass, i.e., the proportions of carbohydrates, proteins and lipids (Charnier et al., 2017). For the analysis, approximately 2 cm³ of freeze-dried and ground samples were transferred into capped crystal vials. To assure homogeneity of the samples, each sample was processed three times in the NIRS, mixed after each measurement. The reported results are the average of the three measurements from the same sample with a standard deviation smaller than 5 %.

2.6. Validating NIRS results using traditional biochemical methane potential test

For one arbitrarily selected biomass sample, the NIRS prediction of BMP was compared to the result of a traditional BMP test. A traditional BMP test was done in triplicate in 500 mL serum bottles, incubated under mesophilic conditions (35 °C), as in Carrère et al., (2009). 5.85 g of freeze-dried OPG biomass (68 % volatile solids/total solids) was added to each bottle, containing 175 mL of anaerobic sludge as inoculum (70 g·L⁻¹ of volatile solids), 4.3 mL of oligo nutrients, 4 mL of metal solution, and 21 mL NaHCO₃ solution (50 g·L⁻¹). Tap water was added to obtain a total volume of 400 mL. The pH was adjusted to 7–8. The solids/biomass ratio of samples was 0.3 g COD of OPG biomass per gram of organic matter from the anaerobic sludge. Biogas volume was measured by liquid displacement and its composition was measured by gas chromatography. A first order k trend function was determined using the modified model of Gompertz (Batstone et al., 2009) to fit BMP (R² = 0.987). The BMP tests was conducted over 90 days until biogas production was indifferent from the negative control, i.e., anaerobic sludge without the addition of OPG biomass.

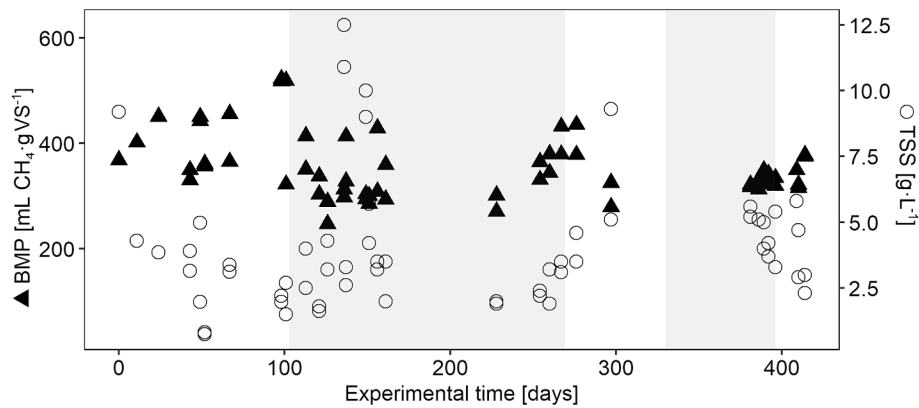


Fig. 2. Measured values of total suspended solids (\circ , TSS) and biochemical methane potential (\blacktriangle , BMP) over experimental time.

2.7. Elemental analysis of photogranular biomass

The elemental analysis for carbon, hydrogen, nitrogen and sulphur (S) contents in samples of total suspended solids were determined in a Flash EA2000 elemental analyzer (Thermo Fisher Scientific, UK) equipped with a Flash EA 1112 flame photometric detector, according to manufacturer's instructions. The oxygen content was then calculated by subtracting from total suspended solids the sum of carbon, hydrogen, nitrogen and sulfur, as well as the ash contents, determined by loss at ignition at 550 °C. The elemental analysis was done on samples immediately before the onset of the starvation experiments and at the end of the experiments.

2.8. Statistical analyses

Data analyses were conducted using R 4.2.3 (R Core Team, 2023). Boxplots were created with the ggplot2 package (Wickham, 2016). Test for association between paired samples (with Pearson's product moment correlation coefficient and Kruskal tests) and two-factor analysis of variance (ANOVA) without replication were computed using R base. A Partial Least Squares (PLS) analysis was carried out between the non-constant parameters (X matrix, explicative variables, e.g., HRT or Load) and the BMP predictions on the 55 samples using the Kernel method in the 'pls' package (Liland et al., 2023). This is particularly efficient when the number of samples is larger than the number of variables, because it is not calculating the cross-product matrix of X. Other parameters were tested but turned out to be highly correlated to others, i.e., cycle length, light-timing (that determines light regime), total solids, volatile solids, total suspended solids and volatile suspended solids. They were thus omitted for the analysis presented here. The coefficient of correlation (R^2) was used to assess the accuracy of the PLS model.

3. Results and discussion

3.1. Benchmarking NIRS method for photogranules

To benchmark BMP predictions from near-infrared spectrometry (NIRS), a traditional BMP test was done in triplicates. After 90 days, the cumulated methane from OPG biomass was 461 ± 9 mL $\text{CH}_4 \cdot \text{gVS}^{-1}$. For the same samples, the NIRS approach estimated a BMP of 450 mL $\text{CH}_4 \cdot \text{gVS}^{-1}$. The difference of 5 % between the two methods, corresponding to values between 5 and 25 mL $\text{CH}_4 \cdot \text{gVS}^{-1}$, depending on the sample's BMP, is much less than the intrinsic errors of the methods themselves (Holliger et al., 2016). This confirms that the statistical model approximates well the traditional BMP also for photogranule biomass. The benchmark was necessary since the original model for NIRS data was trained with a wide range of biomass, including

phototrophic biomass but not OPGs (Lesteur et al., 2011). All BMP values in this study were consequently obtained using the rapid NIRS approach.

3.2. Highest biochemical methane potential for photogranules

In Fig. 3, the BMPs obtained in this manuscript are compared to literature values for other types of biomass related to wastewater treatment or to constituents of the microbial community of OPGs. Details from the literature studies are given in the Supplementary material. Compared to the literature, the BMPs obtained from the two replicated SBRs were highest with an average of 354 ± 11 and 358 ± 12 mL $\text{CH}_4 \cdot \text{gVS}^{-1}$, respectively ("OPG" in Fig. 3). There is no statistical difference between the biomass from the two reactors (p-value = 0.34, Kruskal test).

Photogranules are a candidate biomass for wastewater treatment. For this reason, their BMP was compared to biomass from the current reference process for wastewater treatment, the conventional activated sludge process. The average BMP of 219 ± 54 mL $\text{CH}_4 \cdot \text{gVS}^{-1}$ of activated sludge ("CAS" in Fig. 3) is significantly lower than for OPGs (p-value ≤ 0.001 , Kruskal test). The potential to recover energy from OPG biomass is around 60 % higher than for activated sludge (Fig. 3).

Photogranules may be imagined as a mixture of an activated sludge community with phototrophic organisms, i.e., algae and cyanobacteria. It may therefore be that the phototrophic constituents of a photogranule increase their BMP compared to activated sludge. Comparing OPG biomass with phototrophic biomass, it appears that the BMP from OPG is significantly higher than the BMP from algae or cyanobacteria, whether they originate from miscellaneous environments ("Cyanobacteria A" in Fig. 3) or whether they were isolated from photogranules ("Cyanobacteria B") (p-value ≤ 0.001 , Kruskal test). An arithmetic mix of BMPs from activated sludge and phototrophic biomass therefore cannot produce the observed higher BMP of photogranules.

Other heterotrophic-phototrophic assemblages have been studied in the literature, among them microalgal-bacterial flocs (MaB-floc) (van den Hende et al., 2015, 2016) and microalgal-bacterial aggregates (MABA) (Arcila and Buitrón, 2016). These types of biomass were often dominated by eukaryotic microalgae (van den Hende et al., 2015, 2016; Arcila and Buitrón, 2016). The supposed functioning of these types of biomass centers around syntrophic interactions between the two major groups of organisms and is similar to what is postulated for photogranules. The major difference between these assemblages and photogranules is their spatial structure and the frequent dominance of filamentous cyanobacteria in OPGs. Assemblages of heterotrophic bacteria and phototrophic organisms can grow as suspensions, e.g., individual cells or assemblages of some cells, typically difficult to settle by gravity ("Suspended" in Fig. 3) with an average BMP of 178 ± 17 mL $\text{CH}_4 \cdot \text{gVS}^{-1}$ or as aggregates of various forms (e.g., flocs, granules,

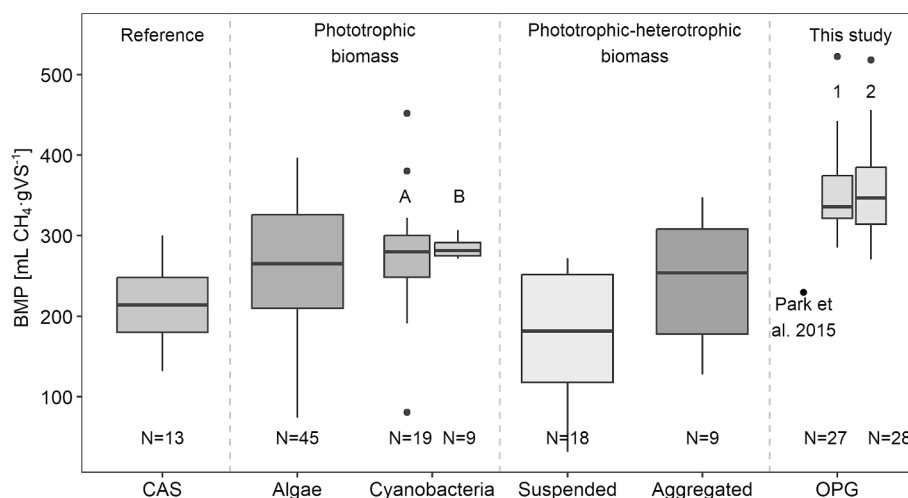


Fig. 3. Comparison of biochemical methane potentials of different types of biomass. Literature values for BMP for conventional activated sludge (CAS) as reference; monoalgal non-marine eukaryotic algae (Algae); monoalgal cyanobacteria (Cyanobacteria), either from various environments (A) or isolated from OPGs (B); non-aggregated phototrophic-heterotrophic cultures (Suspended); aggregated phototrophic-heterotrophic cultures (Aggregates). Data for photogranules from this study are labeled OPG and differentiated by the replicated reactors 1 and 2. The only known literature value for photogranules is added to the OPG and clearly identified. All literature values are provided in the supplementary material.

“Aggregated” in Fig. 3) with an average BMP of $242 \pm 28 \text{ mL CH}_4 \cdot \text{gVS}^{-1}$. For both types of biomass, the average BMP is significantly lower than for OPGs (p -value ≤ 0.000 , Kruskal test). One notable study discussing aggregated biomass reports an exceptionally high BMP value of $348 \text{ mL CH}_4 \cdot \text{gVS}^{-1}$ (Arcila and Buitrón, 2016), similar to what was found for OPGs in this study. According to the description in the article, this type of biomass shares several properties of OPG biomass. It may therefore be that the spatial organization of the biomass is linked to elevated BMPs. However, the first and so far only report of a BMP for true OPG biomass by Park et al. (2015) does not support this hypothesis as it is with a value of $230 \text{ mL CH}_4 \cdot \text{gVS}^{-1}$ well below the average BMP of OPGs reported here. These results suggest that high BMPs from OPG biomass are due to their particular growth form and are not simply caused by a combination of heterotrophic and phototrophic microorganisms.

Placing biomass into the two categories “Suspended” and “Aggregated” (Fig. 3) on the basis of a qualitative description in the literature is an oversimplification of a complex situation and holds the risk of misclassification. In the worst case, this may result in an erroneous detection of

significant differences with OPGs. To avoid misclassification, in the category “Aggregated”, only samples that correspond to the following quantitative criteria were placed: a sludge volume index after 30 min of settling (SVI_{30}) smaller than 150 or a Zone Settling Velocity (ZSV) greater than $1 \text{ m} \cdot \text{h}^{-1}$. Typical SVI_{30} values for activated sludge are between 300 and 400 $\text{mL} \cdot \text{gTSS}^{-1}$ with a ZSV between 0.1 and $0.2 \text{ m} \cdot \text{h}^{-1}$ (Abouhend et al., 2018). “Aggregated” biomass therefore settles more easily than activated sludge (Arcila and Buitrón, 2016; Van den Hende et al., 2016). The samples in the “Suspended” category are assumed to not settle better than a typical activated sludge, based on their descriptions in the respective publications.

3.3. Effect of starvation on BMP of photogranules

The effect of the starvation periods on BMP was tested for photogranular biomass. During the starvation periods, the organic carbon provided in the feed of the two photobioreactors was reduced and in one case eliminated from the feed for three consecutive days (Table 2). This experiment was repeated three times at about one-month intervals. The

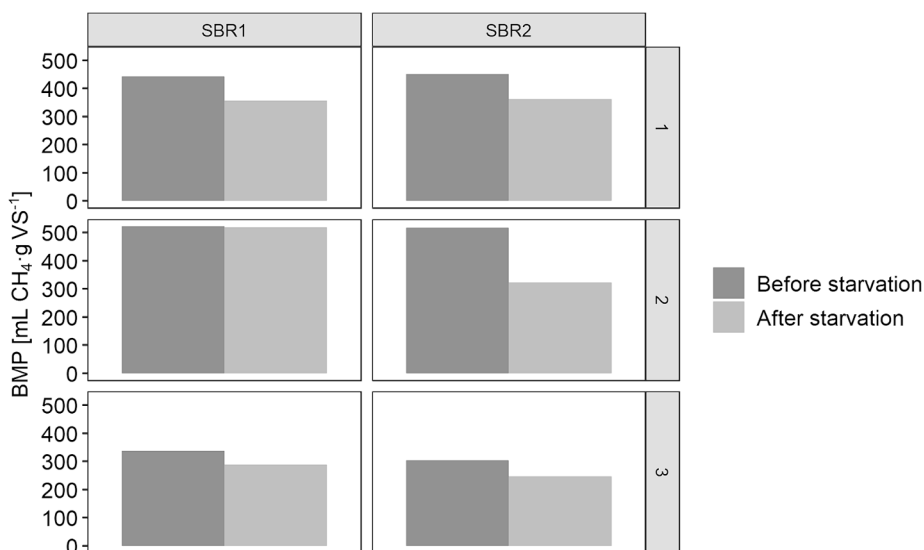


Fig. 4. BMP of OPG biomass before and after three days of starvation in two independently operated reactors during three independent experiments. The average BMP decreased after starvation (ANOVA with “reactor” and “experiments” as factors, p -value = 0.02).

six datasets (two reactors \times three experiments) were analyzed using ANOVA blocking the factors “reactor” and “experiment”. A decrease of BMP of on average $80 \pm 11 \text{ mL CH}_4 \cdot \text{gVS}^{-1}$ (-18.6 %) after starvation was detected (ANOVA test, p-value = 0.02) (Fig. 4). The pre-starvation level of BMP was recovered about 10 days after normal operation was picked up again. These changes in BMP suggest a cycle of production and consumption of storage compounds in OPG biomass.

The relative proportions of proteins, carbohydrates and lipids of the feedstock have an impact on the digestion performance. Excessively high concentrations of any of these fractions lead to the release or accumulation of secondary products that inhibit methanogens (Hagos et al., 2017; Cuellar-Bermudez et al., 2019). Therefore, it is important to consider the macromolecular composition of a feedstock for anaerobic digestion. In cyanobacteria, the macromolecular composition highly depends on nutrient supply (Cuellar-Bermudez et al., 2019). It is thus expected that the BMP of OPGs depends on the nutrient supply. To test whether a decrease in BMP after starvation was associated with a change in the biochemical composition of the biomass, the macromolecular composition of the OPG biomass before and after starvation was compared. The proportions of carbohydrates, lipids and proteins of photogranules were predicted using NIRS. Photogranule biomass was composed of on average $19.6 \% \pm 14.3 \%$ carbohydrates, $67.5 \% \pm 8.4 \%$ proteins and $12.9 \% \pm 13.3 \%$ lipids, resulting in a protein to carbohydrate ratio of 3.4. No change was detected before and after starvation. The elemental analysis reveals the molecular formula of the biomass (carbon, hydrogen, oxygen, nitrogen and sulfur composition) from which the C/N ratio can be calculated. The C/N ratio did not change before and after starvation of experiments 1 and 2 (ANOVA test, p-value = 0.37) (Table 2). However, for starvation experiment 3, the C/N ratio decreased from 4.2 to 2.9 for SBR-1 and from 4.5 to 3.4 for SBR-2 (Table 2), indicating a relative increase of nitrogen content in the biomass. Fixation of atmospheric nitrogen by some cyanobacteria such as *Oscillatoria* sp. is possible under shortage of other nitrogen sources (Benemann, 1979; Gallon, 2001; Markou et al., 2014). Since nitrogen and organic carbon are absent in the feed solution used in the third starvation cycle, N_2 and CO_2 fixation are possible. N_2 fixation comes at a high ATP cost (Großkopf and LaRoche, 2012). This might explain a higher consumption of carbon-rich storage compounds, resulting in a lower C/N and lower BMP. The correlation between the macromolecular composition of OPG biomass obtained by NIR spectroscopy and the chemically measured elemental composition may reveal interesting dynamics possibly adding a relatively simple and fast measure to assess the suitability of a specific type of OPG biomass for methane production. At the

same time, it is important to recall that a BMP is normalized by mass and represents a property of a type of biomass, but not an absolute quantity. From an energy recovery perspective, it is equally important to consider the amount of biomass (with a specific property) inside a reactor to obtain an absolute amount of methane to be produced. Contrary to what was expected, in some situations, notably the starvation experiment 3, the biomass increased after starvation (Table 2). Therefore, the total volume of methane that could be potentially produced from the biomass contained in the reactors may increase after starvation, despite a decrease in specific BMP (Fig. 5). It is unclear how the biomass, especially in the starvation experiment 3, could increase over time in the absence of a carbon source other than atmospheric CO_2 . After careful checking, measurement errors can be ruled out. It was therefore decided to present the data, as there are at this point no methodological problems identified that justify omitting these points as outliers. To conclude, starvation generally reduces the BMP of OPG biomass grown in SBR. Starvation thus influences the property of the biomass. The changed properties are not reflected by the measurements of the elemental or macromolecular composition of the biomass. The unexpected and so far unexplained biomass increase after starvation offset the reduction in BMP and leads in some cases to an increased potential methane volume when considering the total biomass in the reactor.

3.4. Effect of operation parameters on BMP of photogranules

Operating conditions were deliberately varied over time (Table 1 and Fig. 1) to related their impact on the BMP of the resulting biomass. A PLS analysis was performed to discern the most influential parameters. The tested parameters were light intensity (PAR), light regime (PAR per day), hydraulic retention time (HRT), maximum carbon concentration in SBR cycle, organic carbon load (related to maximum carbon concentration and HRT) and biomass concentration. Every combination of parameters was kept constant over at least three days to insure stable reactor behavior. The results from the PLS analysis are presented as principal component plot in Fig. 6. The PLS model encompassed the variance in the BMP data with a correlation of 40 %, indicating that other parameters may exist that correlate with BMP but were not considered in this study. Among the parameters tested in this study, organic carbon load (‘Load’ in Fig. 6) and its maximum concentration (‘maxCOD’) positively correlated with BMP (Pearson correlations $\text{cor} = 0.566$, p-value < 0.001 for Load and $\text{cor} = 0.573$, p-value < 0.001 for maxCOD respectively). The carbon load was therefore the more influential reactor parameter on BMP. On the other hand, the biomass

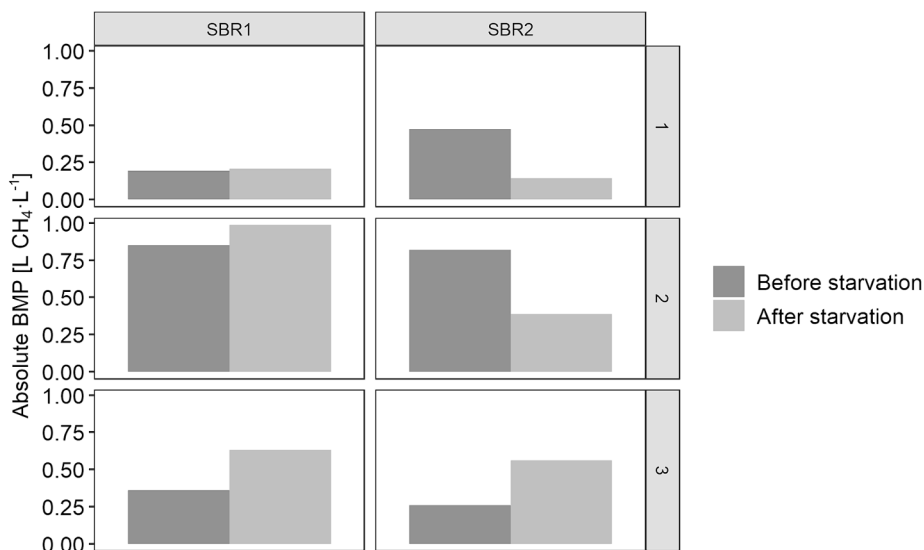


Fig. 5. Expected methane volume per volume unit of the reactor, considering BMP and biomass concentration before and after starvation. This measure can be interpreted as an absolute BMP. The data are separated by reactor (SBR 1 and 2) and starvation experiments 1–3.

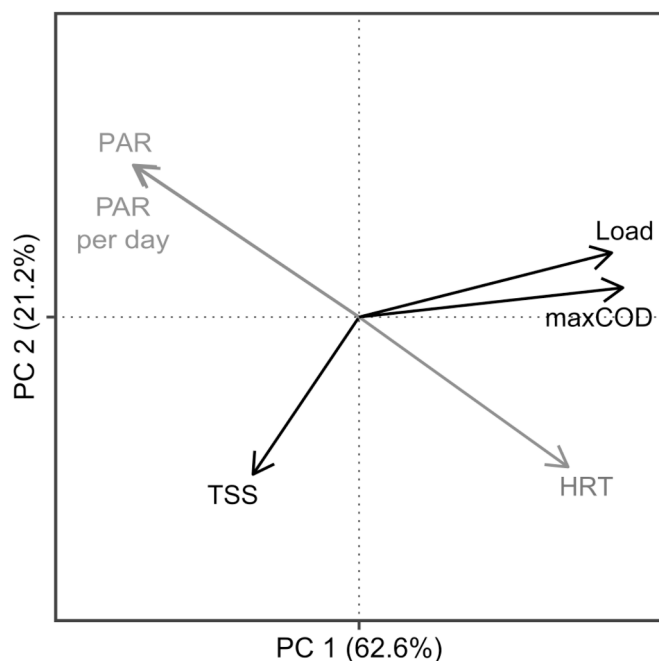


Fig. 6. Biplot of the PLS analysis from BMP values. Black arrows (statistically significant) and grey arrows (statistically not significant) indicate reactor descriptors that varied among samples: light intensity (PAR), light regime (PAR per day), biomass concentration (TSS), hydraulic retention time (HRT), maximum carbon peak which is obtained at the beginning of every cycle (maxCOD) and organic carbon load (Load). Principal components 1 in x-axis (62.6%) and 2 in y-axis (21.2%) explained a total of 84% of the variance on BMP with a correlation of 40%.

concentration (TSS in Fig. 6) was negatively correlated to BMP (Pearson correlation $cor = -0.361$, p -value < 0.05). This may be caused by a lower specific load at higher biomass concentrations, or adverse effects caused by reduced light penetration into the reactor (Gernigon et al., 2019). Determining the optimal biomass concentration and carbon load for maximizing energy recovery of the excess biomass will be a future challenge towards the development of a photogranule-based bioprocess.

The HRT was not significantly correlated to BMP, in contrast to other studies. In Arcila and Buitrón (2016), the highest methane yield ($348 \text{ mL CH}_4 \cdot \text{gVS}^{-1}$) was obtained at the longest HRT of 10 days, compared to 2 and 6 days HRT, for microalgae-bacteria granules grown in a high-rate algal ponds. Results from Arcila and Buitrón (2016) and from this study were however not directly comparable since SBR operation allows much shorter HRTs ($< 8\text{h}$) due to the uncoupling of HRT from solids retention time (SRT). On the other hand, van den Hende et al. (2016) reported a decrease of BMP of 13.8 % after increasing the SRT in a microalgae-bacteria flocs system grown in high-rate algal ponds and fed with food-industry effluent. The effects of SRT and HRT on BMP varied a lot between studies, but range of variations of these operating parameters also differed greatly between studies, making comparisons difficult. In any case, varying SRT or HRT may possibly induce the growth of a biomass with altered biochemical composition leading to different BMP values.

Further research is essential to unravel the interplay between photobioreactor operation, the accumulation of storage compounds in biomass, and the subsequent energy recovery from the biomass. Although OPG biomass has been identified as a promising candidate for future applications in wastewater treatment, a significant knowledge gap remains in terms of biotechnological applications and the valorization of biomass. This study marks an initial stride towards the understanding of modulation of the energy recovery potential from OPG biomass.

4. Conclusions

This study showed that oxygenic photogranules (OPGs) grown on wastewater in SBR have on average a higher BMP ($356 \text{ mL CH}_4 \cdot \text{gVS}^{-1}$) than related biomass from other sources. It seems that more highly structured phototrophic-heterotrophic biomass creates conditions that leads to an elevated BMP. The effect of photobioreactor operation on BMP was identified. Carbon load had the greatest effect among the six operational parameters tested. Conversely, starving OPGs for three days significantly decreased the BMP by 18.6 % on average ($80 \text{ mL CH}_4 \cdot \text{gVS}^{-1}$). As final conclusion, load conditions can modulate BMP of OPG biomass.

CRedit authorship contribution statement

Sandra Galea-Outón: Writing – original draft, Visualization, Methodology, Formal analysis, Data curation, Conceptualization. **Kim Milferstedt:** Writing – review & editing, Visualization, Validation, Supervision, Methodology, Conceptualization. **Jérôme Hamelin:** Writing – review & editing, Validation, Supervision, Project administration, Methodology, Conceptualization.

Declaration of competing interest

The authors declare that they have no known competing financial interests or personal relationships that could have appeared to influence the work reported in this paper.

Data availability

Data will be made available on request.

Acknowledgments

The authors gratefully acknowledge H el ene Carr ere and Jimin Kim for assisting in BMP experiments, to Eric Latrille for his help in interpreting NIR spectra and to R emi Servien for his help in interpreting PLS analysis.

Funding

Sandra Galea-Out on was funded by MICA-HOLOFLUX metaprogram from INRAE and by R egion Occitanie, France. This work was supported by SEP-CONACYT-ANUIES-ECOS NORD Project (Mexico 296514/France M18A01). This work benefited from the Environmental Biotechnology and Biorefinery Facility (Bio2E) of INRAE-LBE (<https://doi.org/10.15454/1.557234103446854E12>).

Appendix A. Supplementary data

Supplementary data to this article can be found online at <https://doi.org/10.1016/j.biortech.2024.130986>.

References

- Abouhend, A.S., McNair, A., Kuo-Dahab, W.C., Watt, C., Butler, C.S., Milferstedt, K., Hamelin, J., et al., 2018. The oxygenic photogranule process for aeration-free wastewater treatment. *Environ. Sci. Technol.* 52, 3503–3511.
- Angelidaki, I., Alves, M., Bolzonella, D., Borzacconi, L., Campos, J.L., Guwy, A.J., Kalyuzhnyi, S., et al., 2009. Defining the biomethane potential (BMP) of solid organic wastes and energy crops: A proposed protocol for batch assays. *Water Sci. Technol.* 59, 927–934.
- Appels, L., Baeyens, J., Degr eve, J., Dewil, R., 2008. Principles and potential of the anaerobic digestion of waste-activated sludge. *Prog. Energy Combust. Sci.* 34, 755–781.
- Arcila, J.S., Buitr on, G., 2016. Microalgae-bacteria aggregates: effect of the hydraulic retention time on the municipal wastewater treatment, biomass settleability and methane potential. *J. Chem. Technol. Biotechnol.* 91, 2862–2870.

- Batstone, D.J., Tait, S., Starrenburg, D., 2009. Estimation of hydrolysis parameters in full-scale anaerobic digesters. *Biotechnol. Bioeng.* 102, 1513–1520.
- Benemann, J.R., 1979. Production of nitrogen fertilizer with nitrogen-fixing blue-green algae. *Enzyme Microb. Technol.* 1, 83–90.
- Brockmann, D., Gérard, Y., Park, C., Milferstedt, K., Hélias, A., Hamelin, J., 2021. Wastewater treatment using oxygenic photogranule-based process has lower environmental impact than conventional activated sludge process. *Bioresour. Technol.*, 319.
- Carrère, H., Sialve, B., Bernet, N., 2009. Improving pig manure conversion into biogas by thermal and thermo-chemical pretreatments. *Bioresour. Technol.* 100, 3690–3694.
- Charnier, C., Latrille, E., Jimenez, J., Lemoine, M., Boulet, J.C., Miroux, J., Steyer, J.P., 2017. Fast characterization of solid organic waste content with near infrared spectroscopy in anaerobic digestion. *Waste Manag.* 59, 140–148.
- Cuellar-Bermudez, S.P., Magdalena, J.A., Muylaert, K., Gonzalez-Fernandez, C., 2019. High methane yields in anaerobic digestion of the cyanobacterium *Pseudanabaena* sp. *Algal Res.* 44, 101689.
- Gallon, J.R., 2001. N₂ fixation in phototrophs: Adaptation to a specialized way of life. *Plant Soil.* 230, 39–48.
- Gernigon, V., Chekroun, M.A., Cockx, A., Guiraud, P., Morchain, J., 2019. How mixing and light heterogeneity impact the overall growth rate in photobioreactors. *Chem. Eng. Technol.* 42, 1663–1669.
- Großkopf, T., LaRoche, J., 2012. Direct and indirect costs of dinitrogen fixation in *Crocospira watsonii* WH8501 and possible implications for the nitrogen cycle. *Front. Microbiol.* 3, 1–10.
- Hagos, K., Zong, J., Li, D., Liu, C., Lu, X., 2017. Anaerobic co-digestion process for biogas production: Progress, challenges and perspectives. *Renew. Sustain. Energy Rev.* 76, 1485–1496.
- Holliger, C., Alves, M., Andrade, D., Angelidaki, I., Astals, S., Baier, U., Bougrier, C., et al., 2016. Towards a standardization of biomethane potential tests. *Water Sci. Technol.* 74, 2515–2522.
- Latrille, E., Lesteur, M., Preys, S., Roussel, S., Steyer, J.-P., Boulanger, A., Treguer, R., et al., 2013. Fast prediction of biochemical methane potential (BMP) of organic waste by near infra-red spectroscopy. In: NIR 2013 - 16th International Conference on Near Infrared Spectroscopy. Institut National de Recherche en Sciences et Technologies pour l'Environnement et l'Agriculture (IRSTEA), La Grande Motte, France.
- Lesteur, M., Latrille, E., Maurel, V.B., Roger, J.M., Gonzalez, C., Junqua, G., Steyer, J.P., 2011. First step towards a fast analytical method for the determination of Biochemical Methane Potential of solid wastes by near infrared spectroscopy. *Bioresour. Technol.* 102, 2280–2288.
- Liland, K.H., Bjørn-Helge, M. & Wehrens, R. 2023. Pls: Partial Least Squares and Principal Component Regression. R package version 2.8-2.
- Lipps, W., Baxter, T. & Braun-Howland, E. 2017. 2540 solids in: standard methods for the examination of water and wastewater. Stand. Methods Comm. Am. Public Heal. Assoc. Am. Water Work. Assoc. Water Environ. Fed. 2:55–61.
- Markou, G., Vandamme, D., Muylaert, K., 2014. Microalgal and cyanobacterial cultivation: The supply of nutrients. *Water Res.* 65, 186–202.
- Milferstedt, K., Kuo-Dahab, W.C., Butler, C.S., Hamelin, J., Abouhend, A.S., Stauch-White, K., McNair, A., et al., 2017. The importance of filamentous cyanobacteria in the development of oxygenic photogranules. *Sci. Rep.* 7, 1–15.
- Park, C., Sauvenheav, L., Sialve, B., Carrère, H., 2015. The anaerobic digestibility of algal-sludge granules. *Water Environment Federation Residuals and Biosolids*, Washington DC, USA.
- Pronk, M., de Kreuk, M.K., de Bruin, B., Kamminga, P., Kleerebezem, R., van Loosdrecht, M.C.M., 2015. Full scale performance of the aerobic granular sludge process for sewage treatment. *Water Res.* 84, 207–217.
- van den Hende, S., Beyls, J., De Buyck, P.J., Rousseau, D.P.L., 2016. Food-industry-effluent-grown microalgal bacterial flocs as a bioresource for high-value phytochemicals and biogas. *Algal Res.* 18, 25–32.
- Van den Hende, S., Beelen, V., Julien, L., Lefoulon, A., Vanhoucke, T., Coolsaet, C., Sonnenholzner, S., et al., 2016. Technical potential of microalgal bacterial floc raceway ponds treating food-industry effluents while producing microalgal bacterial biomass: An outdoor pilot-scale study. *Bioresour. Technol.* 218, 969–979.
- van den Hende, S., Laurent, C. & Bégué, M. 2015. Anaerobic digestion of microalgal bacterial flocs from a raceway pond treating aquaculture wastewater: Need for a biorefinery. *Bioresour. Technol.*
- van der Roest, H.F., de Bruin, L.M.M., Gademan, G., Coelho, F., 2011. Towards sustainable waste water treatment with Dutch Nereda® technology. *Water Pract. Technol.* 6, 3–6.